Biogeosciences Discuss., 9, 2709–2753, 2012
www.biogeosciences-discuss.net/9/2709/2012/
doi:10.5194/bgd-9-2709-2012

Biogeosciences Discussions

Distributions of the carbonate system properties, anthropogenic CO_2, and acidification during the 2008 BOUM cruise (Mediterranean Sea)

F. Touratier[1], V. Guglielmi[1], C. Goyet[1], L. Prieur[2], M. Pujo-Pay[3], P. Conan[3], and C. Falco[1]

[1]IMAGES, Université de Perpignan, 52 avenue Paul Alduy, 66860 Perpignan, France
[2]LOV, Quai de la darse, B.P. 28, 06234 Villefranche sur mer, France
[3]Laboratoire d'Océanographie Microbienne, CNRS, UMR7621, Observatoire Océanologique, 66651 Banyuls/mer, France

Received: 17 February 2012 – Accepted: 17 February 2012 – Published: 12 March 2012

Correspondence to: F. Touratier (touratier@univ-perp.fr)

Published by Copernicus Publications on behalf of the European Geosciences Union.

Abstract

We relate here the distributions of two carbonate system key properties (total alkalinity, A_T; and total dissolved inorganic carbon, C_T) measured along a section in the Mediterranean Sea, going from Marseille (France) to the south of the Cyprus Island, during the 2008 BOUM cruise. The three main objectives of the present study are (1) to draw and comment on the distributions of A_T and C_T in the light of others properties like salinity, temperature, and dissolved oxygen, (2) to estimate the distribution of the anthropogenic CO_2 (C_{ANT}) in the intermediate and the deep waters, and (3) to calculate the resulting variation of pH (acidification) since the beginning of the industrial era. Since the calculation of C_{ANT} is always an intense subject of debate, we apply two radically different approaches to estimate C_{ANT}: the very simple method TrOCA and the MIX approach, the latter being more precise but also more difficult to apply. A clear picture for the A_T and the C_T distributions is obtained: the mean concentration of A_T is higher in the oriental basin while that of C_T is higher in the occidental basin of the Mediterranean Sea, fully coherent with the previous published works. Despite of the two very different approaches we use here (TrOCA and MIX), the estimated distributions of C_{ANT} are very similar. These distributions show that the minimum of C_{ANT} encountered during the BOUM cruise is higher than 46.3 µmol kg^{-1} (TrOCA) or 48.8 µmol kg^{-1}(MIX). All Mediterranean water masses (even the deepest) appear to be highly contaminated by C_{ANT}, as a result of the very intense advective processes that characterize the recent history of the Mediterranean circulation. As a consequence, unprecedented levels of acidification are reached with an estimated decrease of pH since the pre-industrial era of −0.148 to −0.061 pH unit, which places the Mediterranean Sea as one of the most acidified world marine ecosystem.

BGD
9, 2709–2753, 2012

1 Introduction

Oceanographic cruises throughout the whole Mediterranean Sea where high quality measurements of the carbonate system properties have been carried out are very uncommon. Until recently, the sole existing cruise with such measurements was the 2001 German cruise M51/2 on board the R/V *Meteor*. The analysis of the cruise results allowed us to draw for the first time the Mediterranean east-west distribution for total alkalinity (A_T, $\mu mol\,kg^{-1}$; see Schneider et al., 2007) and total dissolved inorganic carbon (C_T; $\mu mol\,kg^{-1}$), to estimate the concentration of anthropogenic CO_2 (Scnheider et al., 2010; Touratier and Goyet, 2011), and to provide the range of acidification reached by the Mediterranean waters since the pre-industrial era (Touratier and Goyet, 2011). The latter study shows that all water masses in the Mediterranean Sea (even the deepest) are already acidified with a pH decrease from −0.14 to −0.05, which places the Mediterranean Sea among the most acidified marine ecosystems. Comparatively, the acidification in the world ocean surface layer reaches −0.1, while most deep waters are not yet acidified (Orr et al., 2005; Martin et al., 2008).

The increase of acidification in seawater is mainly governed by the accumulation of anthropogenic CO_2 (C_{ANT} thereafter). At this point, we face two major constraints: (1) C_{ANT} cannot be measured since atoms of carbon (or oxygen) from natural or anthropogenic origin cannot be distinguished, and (2) the concentration of C_{ANT} represents only a very small percentage (0–2 %) of C_T. This implies that C_{ANT} is indirectly estimated using model(s) whose complexity may vary from a simple equation (the TrOCA approach; Touratier et al., 2007) to a full 3-D model (e.g. Gerber et al., 2009). An important criterion to select a valuable approach is its accuracy to estimate C_{ANT} which ideally should remain below $\pm 10\,\mu mol\,kg^{-1}$.

Recently, using the same 2001 Meteor 51/2 dataset, the papers published by Schneider et al. (2010) and Touratier and Goyet (2011) provided different C_{ANT} estimates. Despite a very similar pattern obtained in the distributions of C_{ANT}, it exist a bias of $\sim 20\,\mu mol\,kg^{-1}$ between the two estimates (the highest is from Touratier and Goyet,

BGD
9, 2709–2753, 2012

2011). This is a direct consequence of the method chosen by the authors: Schneider et al. (2010) used the transit time distribution (TTD) approach, while Touratier and Goyet (2011) applied the TrOCA approach. We estimate that such uncertainty on C_{ANT} significantly affects the estimated level of acidification by ±25 %.

In the present study, we use new results available from the 2008 BOUM French cruise (Biogeochemistry from the Oligotrophic to the Ultra oligotrophic Mediterranean Sea). The results of the measurements of key properties like C_T and A_T from this cruise allow us to obtain a complete picture of the carbonate system properties for the Mediterranean Sea during the year 2008.

Our first objective is to describe the distribution of the main water masses along the east-west section of the BOUM cruise using conservative properties like salinity and temperature. The 2008 distributions of the carbonate system properties (A_T, C_T) will be then discussed in the light of the water masses physical properties, and the dissolved oxygen concentration (second objective). The third objective is to estimate C_{ANT} using both the MIX (Goyet et al., 1999) and the TrOCA (Touratier et al., 2007) approaches. Our final objective is to draw a map of the acidification induced by the accumulation of C_{ANT} in the Mediterranean Sea since the beginning of the industrial era.

2 Study area and sampling

The BOUM cruise (Biogeochemistry from the Oligotrophic to the Ultra oligotrophic Mediterranean Sea; http://www.com.univ-mrs.fr/BOUM/) occurred during summer 2008, from 20 June to 22 July, on board the R/V *L'Atalante*. The specific objectives of the INSU/CNRS BOUM project (which is also part of the European SESAME project) are detailed in Moutin et al. (2012). It consists of a longitudinal transect (more than 3000 km long from the Levantine basin to the Northwestern Mediterranean Sea; see Fig. 1) of 27 short-term stations and 3 long-term stations (4 days; stations A, B, and C) which provide the distribution of the relevant physical and biogeochemical properties from surface to bottom. The long-term stations A, B, and C are located in the center

BGD
9, 2709–2753, 2012

of anticyclonic gyres (located in the Algero-Provencal, the Ionian, and the Levantine basins, respectively) where horizontal advection was expected to be low.

In the present paper, we use the following properties: potential temperature (θ; °C), salinity (S), dissolved oxygen (O_2; µmol kg^{-1}), nitrates (NO_3; µmol kg^{-1}), phosphates (PO_4; µmol kg^{-1}), silicates (SiO_4; µmol kg^{-1}), total alkalinity (A_T; µmol kg^{-1}), and total dissolved inorganic carbon (C_T; µmol kg^{-1}). Note however that all these properties are not available at all sampling depths.

Profiles for θ, S (conductivity), and O_2 were obtained using a Sea-Bird Electronics 911 PLUS CTD system. Each CTD cast was associated with a carousel of 24 Niskin bottles to collect seawater samples used to perform the analysis of the other chemical and biological properties. Concerning the nutrients (NO_3, PO_4, and SiO_4), the description of the methods used for the analysis are explained in Pujo-Pay et al. (2011) and Crombet et al. (2011). For A_T and C_T measurements, seawater samples were collected into washed 500 ml borosilicate glass bottles, and poisoned with a saturated solution of $HgCl_2$. At the end of the cruise, the samples were sent back to the laboratory at the University of Perpignan for analysis. The measurements of A_T and C_T were performed by potentiometric titration using a closed cell, as described in details in the handbook of methods for the analysis of the various parameters of the CO_2 system in seawater (DOE, 1994).

3 Distribution of the physical properties and dissolved oxygen

The distributions of S and θ along the 2008 BOUM transect are shown in Fig. 2a and b, respectively. These distributions reflect the current knowledge on the 3 layered system that characterizes the Mediterranean Sea. With the help of the θ/S diagrams for the Western (Fig. 3a) and the Eastern (Fig. 4a) basins, we first identify the upper layer (0–300 m) where is located the Modified Atlantic Water (MAW). The origin of MAW is the surface Atlantic Ocean water that enters the Mediterranean Sea through the Strait of Gibraltar. Along its complex circulation pattern from West to East, MAW gains in both

BGD
9, 2709–2753, 2012

S and θ as a consequence of the negative precipitation-evaporation balance and the increasing warming up of the sea surface. The Mediterranean intermediate layer (300–1000 m) is occupied by essentially two water masses: the Winter Intermediate Water (WIW) which results from moderate winter cooling of the surface layer, endemic to the Western basin; and the Levantine Intermediate Water (LIW) that spreads everywhere in the Mediterranean Sea from its formation site which is located in the Levantine Sea. The upper and the intermediate layers, and their associated water masses, form an open thermohaline cell which exchanges seawater and properties with the Atlantic Ocean.

At depths greater than ca. 1000 m, the Western and the Eastern basins are filled with very different but relatively isolated deep waters. During the period 1990–1992, the Eastern Mediterranean Transient (EMT) radically modified the distribution of the water masses in the Eastern basin. The EMT was induced by a combination of meteorological and hydrological factors which caused the Aegean Sea (Fig. 1) to become a new source of deep water in addition to the Adriatic source, which traditionally feeds the Eastern Mediterranean Deep Water (EMDW; see Roether et al., 1999; Klein et al., 1999; Lascaratos et al., 1999; Theocharis et al., 2002). Rubino and Hainbucher (2007) note however that the Adriatic Sea has returned to represent a major role in the formation of the EMDW. In the present paper, we make a distinction between the two types of EMDW according to their origin since they have different S and θ signatures (see the Fig. 4a and the close-up in Fig. 4b): the EMDW originating from the Adriactic Sea and the Aegean Sea are referred here by the acronyms $EMDW_{Adr}$ and $EMDW_{Aeg}$, respectively.

Mainly two water masses occupy the deepest part of the Western basin: the Tyrrhenian Deep Water (TDW) and the Western Mediterranean Deep Water (WMDW), see Fig. 3a and b. According to Millot et al. (2006), the TDW results from a mixing between the Eastern Overflow Water (EOW) and the WMDW that travels up to the Tyrrhenian Sea *via* the Sardinia Channel (the contribution of water masses may vary in time). The TDW then exits the Tyrrhenian Sea using the Sardinia Channel (but in the opposite

BGD
9, 2709–2753, 2012

direction) to invade large portions of the Algero-Provencal basin. Since the density of the TDW is slightly lower than that of the WMDW, the former is located above the latter in the water column.

When compared to the distributions of S and θ obtained during the 2001 Meteor cruise (Touratier and Goyet, 2011; see their Figs. 3d and 4d, respectively), those of the 2008 BOUM cruise indicate that the overall distribution of intermediate and deep water masses of the Mediterranean Sea did not changed significantly.

The distribution of the O_2 concentration along the BOUM section is shown in Fig. 2c. The intermediate depths are occupied by a layer where O_2 is $<185\,\mu mol\,kg^{-1}$. The thickness of this layer is ~600 m and it sinks approximately from a mean depth of 300 m in the West to 700 m in the East. In this O_2 minimum layer, the lowest concentrations ($<175\,\mu mol\,kg^{-1}$) are found in the Algero-Provencal basin.

The O_2 concentration increases with depth in both the Western and the Eastern basin. Close to the bottom, concentrations of $\sim195\,\mu mol\,kg^{-1}$ indicate that some recent invasions of dense and O_2-rich waters has occurred as a consequence of deep water formation processes that potentially produced new volumes of WMDW, $EMDW_{Adr}$ and $EMDW_{Aeg}$. The 2008 O_2 distribution (Fig. 2c) is very similar to the one observed in 2001 during the Meteor cruise (see Fig. 7d in Touratier and Goyet, 2011). Only minor changes occurred in intermediate and deep waters over a 7 yr period, like an overall but small decrease of O_2 (a few $\mu mol\,kg^{-1}$) which could results from mixing and consumption of O_2 due to the oxidation of the dissolved organic matter.

4 Distribution of the carbonate system properties

The distribution of the C_T property (Fig. 5a) shows that the highest concentrations ($>2320\,\mu mol\,kg^{-1}$) are generally found in the Western basin. Since this basin contains in average the youngest waters, it has been shown by Touratier and Goyet (2011) that the high level of C_T could essentially result from the accumulation of C_{ANT}. With

BGD
9, 2709–2753, 2012

increasing depths, the rising levels of C_T are a direct consequence of the CO_2 released by the respiration of organisms and the decomposition of organic matters. The C_T distributions for the years 2001 (Touratier and Goyet, 2011) and 2008 are globally similar, but we note a significant increase of ~5–10 µmol kg^{-1} in the intermediate and deep waters in the Eastern basin. For the Western basin, no significant increase or decrease is detected, but it is difficult to give any conclusion since only three stations were sampled for the whole Western Mediterranean Sea during the year 2001. Another interesting characteristic of the 2008 results (Fig. 5a) is the high levels reached by C_T in the area corresponding to station A (Fig. 1, the distance is ~400–500 km from Marseille) where an important anti-cyclonic gyre was identified and studied. Is this 3-D complex structure responsible for an important pumping of C_T with the resulting consequence of the local increase of both C_{ANT} and acidification? If true, the regular occurrence of such gyres throughout the whole Mediterranean Sea could represent a significant portion of the total input of anthropogenic CO_2 to the system.

The distribution of the measured A_T is shown in Fig. 5b. As a consequence of its high salinity, the total alkalinity of the Mediterranean Sea is also high (~2600 µmol kg^{-1}). Major inputs of A_T in the system are the rivers and the Black Sea, while the main outputs are the sedimentation of calcium carbonate and the Atlantic Ocean (Schneider et al., 2007). The Eastern basin is clearly characterized by $A_T > 2600$ µmol kg^{-1} while A_T in the Western basin is always <2600 µmol kg^{-1}. The influence of the Modified Atlantic Water (MAW) flowing in the surface layer of the Mediterranean Sea is clearly revealed by a low total alkalinity signature. Compared to the A_T 2001 distribution (Touratier and Goyet, 2011), the 2008 distribution does not differ significantly.

5 Distribution of the anthropogenic CO_2 (C_{ANT})

Recently, Vázquez-Rodríguez et al. (2009) give an overview of several approaches available from the literature to estimate C_{ANT}. Five of the most recent models (ΔC*, Gruber et al., 1996; C^0_{IPSL}, Lo Monaco et al., 2005; TTD, Waugh et al., 2006; TrOCA,

BGD
9, 2709–2753, 2012

Touratier et al., 2007; and the φC_T^0, Vázquez-Rodríguez et al., 2009) were used to perform an inter-comparison exercise of their C_{ANT} estimates using a common and a high quality dataset available for the Atlantic, the Antarctic, and the Arctic Oceans in order to feed the models with the required observations. One of the conclusions is that all methods give similar spatial distributions and magnitude of C_{ANT} between latitude 60° N–40° S, and that some differences are found among the methods in the Southern Ocean and the Nordic Seas. The C_{ANT} total inventories computed with the TrOCA approach for the whole Atlantic Ocean is 51 Pg C; this clearly shows that this approach does not over- or underestimate C_{ANT} since it is well in the range of the inventories computed by the four other methods (from 47 to 67 Pg C).

Several works have shown that the TrOCA approach is easily and successfully applied to a large variety of marine systems; Touratier and Goyet (2004), Touratier et al. (2005), and Vázquez-Rodriguez et al. (2009) used datasets from the Atlantic Ocean; Lo Monaco et al. (2005) and Sandrini et al. (2007) give results of the TrOCA approach for the southern Ocean and Antarctic Ocean; Goyet et al. (2009) computed C_{ANT} using the TrOCA approach in the southern Pacific Ocean; other studies used the TrOCA approach in the Indian Ocean (Touratier et al., 2007; Goyet and Touratier, 2009; Alvarez et al., 2009). Regarding specifically at the Mediterranean Sea, Touratier and Goyet (2009, 2011) were the first to estimate C_{ANT} and to compute the resulting acidification for the Mediterranean Sea. Using data from the DYFAMED site, Touratier and Goyet (2009) showed the decadal evolution of C_{ANT} in the Northwestern Mediterranean Sea from the mid-1990s to the mid-2000s. During the year 2001, the German cruise 51/2 of the R/V *Meteor* provided high quality data of the carbonate system properties along a longitudinal section throughout the whole Mediterranean Sea, from which Touratier and Goyet (2011) were able to estimate the distribution of C_{ANT}. Using the latter database, Schneider et al. (2010) also computed the distribution of C_{ANT} but using the TTD approach that uses the CFC-12 transient tracer. Although similar patterns are generally obtained for the C_{ANT} distributions computed from TrOCA and TTD, it appears that the C_{ANT} minimum found in the oldest water mass (the depth range is ~1000–1500 m)

BGD
9, 2709–2753, 2012

of the Eastern basin is significantly higher with the TrOCA approach (37.5 µmol kg^{-1}) than with the TTD approach (20.5 µmol kg^{-1}). Such difference is surprising since the inter-comparison exercise performed for the Atlantic Ocean (Vázquez-Rodríguez et al., 2009) give similar values for the C_{ANT} total inventories with 48 Pg C and 51 Pg C for the TTD and the TrOCA approach, respectively.

Given the simplicity, the worldwide applicability, the robustness, the accuracy, and the expertise of the TrOCA approach to estimate C_{ANT} within the Mediterranean waters, we choose to apply this method to the BOUM 2008 dataset. The use of another approach to estimate C_{ANT} is of importance to validate/invalidate the previous estimate. Unfortunately, among the five methods tested during the inter-comparison exercise of Vázquez-Rodríguez et al. (2009), the three methods TTD, ΔC^*, φC_T^0 cannot be applied since CFCs were not measured during the 2008 BOUM cruise. Apart from the TrOCA approach , the only potential candidate is the C_{IPSL}^0 method proposed by Lo Monaco et al. (2005). However, this approach overestimates the computation of the C_{ANT} concentration since its C_{ANT} total inventory reached the highest value of 67 Pg C for the Atlantic Ocean (Vázquez-Rodríguez et al., 2009).

The MIX approach developed by Goyet et al. (1999) has been shown to be very persuasive to estimate the distribution of anthropogenic CO_2 in the northern Indian Ocean using the WOCE I1 high quality dataset. Its results have been compared to those computed from the ΔC^* and the TrOCA approaches (see the papers of Coatanoan et al., 2001; and Touratier et al., 2007). The conclusion of this inter-comparison exercise was that the C_{ANT} distributions computed from MIX and TrOCA were much more correlated to those of three measured anthropogenic tracers (CFC-11, $\Delta^{14}C$, and ^3H) than the one computed from the ΔC^* approach. The use of the MIX approach is particularly recommended for regional studies where the distribution of water masses can be clearly defined (this is the case for the Mediterranean Sea). Other arguments like its accuracy and its independence from the TrOCA approach (the hypotheses used and the computation are radically different) further justify our choice to use the MIX approach as a second approach to estimate C_{ANT} in the present paper.

BGD
9, 2709–2753, 2012

5.1 The MIX approach

The MIX approach developed by Goyet et al. (1999) uses a multi-parameter analysis (Tomczak, 1981; Mackas et al., 1987) to quantify the contribution of the different water sources to the observed data. The MIX approach was initially applied to observations made in the northern Indian Ocean using two conservative tracers (S and θ) and two non conservative tracers (O_2 and A_T). In the present study, the Mediterranean observations allow us to use a modified version of the MIX approach with four conservative tracers (S, θ, NO, and PO) which provides additional constraints for the resolution of the system of equations. Broecker (1974) defined the conservative tracers NO and PO as follows:

$$NO = O_2 + R_{ON}NO_3 \quad (1)$$

$$PO = O_2 + R_{OP}PO_4 \quad (2)$$

where NO and PO are composite tracers of the non conservative tracers O_2 and NO_3 (nitrate concentration in $\mu mol\,kg^{-1}$), and O_2 and PO_4 (phosphate concentration in $\mu mol\,kg^{-1}$), respectively. Based on the equation of Redfield et al. (1963) which describes the average photosynthesis and aerobic respiration in the ocean interior, the composite tracers NO and PO were built using the fact that the consumption of oxygen is balanced by the production of nutrients during the processes of respiration and decomposition The two constants R_{ON} and R_{OP} are the ratios of the stoechiometric coefficients (ψ) involved in the Redfield equation ($R_{ON} = \psi O_2/\psi NO_3$; $R_{OP} = \psi O_2/\psi PO_4$). Typical values given by Redfield et al. (1963) are $R_{ON} = 8.6$ and $R_{OP} = 138$ (molar ratios), but these ratios cannot be representative of the Mediterranean waters since Redfield et al. (1963) never used observations from this region. Here R_{ON} and R_{OP} ratios will be specifically estimated for the Mediterranean case using the BOUM database as explained below.

BGD
9, 2709–2753, 2012

The general conservation equation for a conservative tracer (Ω) is given by:

$$\Omega = \sum_{j=1}^{n} k_j \Omega_j \quad (3)$$

where k_j represents the contribution (also called "mixing coefficient") of a water source j, n is the number of water sources in the system, and Ω_j is the value of the conservative tracer for the water source j.

For each seawater sample, where the conservative tracers Ω are either measured (S and θ) or calculated (NO and PO; see Eqs. 1–2), the contributions k_j are estimated after resolving the system of equations with an inverse method and the following constraints:

$$\sum_{j=1}^{n} k_j = 1 \quad \text{(mass conservation)} \quad (4)$$

$$\forall j, 0 \leq k_j \leq 1 \quad (5)$$

The stability of the results is tested by adding thirty random deviations to the values of Ω and the Ω_j which provide at each point a mean solution for each k_j (Goyet et al., 1999).

5.1.1 Determination of the water sources

The different water sources j are typically identified using the conservative tracers S and θ and their corresponding θ/S diagram. In order to lower the number of the water sources (n), the Mediterranean Sea is treated as two independent systems: the Western basin (longitude $\leq$11.5° E) and the Eastern basin (longitude $\geq$15° E). Consequently, the shallow stations 15 to 17 (Fig. 1) located in the Sicily Strait between 115° E and 15° E are ignored when the MIX approach is applied.

BGD
9, 2709–2753, 2012

For each basin, we use ten water sources (n = 10) noted from W1 to W10 for the Western basin, and from E1 to E10 for the Eastern basin. Water sources must be identified among the BOUM samples but the selection of any sample to be representative for a water source is conditioned by the availability of all properties listed in Table 1 (depth, salinity, temperature, nutrient concentrations, oxygen concentration, and carbonate system properties; these properties are inputs for the MIX approach). All water sources are indicated on the corresponding θ/S diagrams of the Western and Eastern basins (see Figs. 3 and 4, respectively). As indicated by Fig. 3 for the Western Mediterranean Sea, the five water masses MAW, WIW, LIW, WMDW, and TDW are best represented by the water sources W1, W5, W7, W9, and W10, respectively. For the Eastern Mediterranean Sea (Fig. 4), the four water masses MAW, LIW, $EMDW_{Adr}$, and $EMDW_{Aeg}$ are typically represented by the water sources E3, E6, E9, and E10, respectively. Other water sources have been used to take into accounts anomalies like gyres (W2, W3, E1, E2) or specific mixing points in the θ/S diagrams.

5.1.2 Determination of the Redfield ratios R_{ON} and R_{OP}

Specific R_{ON} and R_{OP} ratios for the Mediterranean Sea are determined using the NO_3, the PO_4, and the O_2 data collected during the BOUM cruise. In order to apply the MIX approach, the Western and the Eastern basins are treated separately. The relationships between the nutrients and O_2, and their corresponding linear regressions are all shown in Figs. 6 and 7 for the Western and the Eastern basin, respectively. All information related to these regressions (value of the ratios, number of points used in each regression, mean and standard deviation of the residuals, the Pearson correlation coefficient, and the 99 % confidence interval) is gathered in Table 2. The best results for these regressions were obtained after considering two different layers for both the Western and the Eastern basins: the surface/intermediate layer (from 50 up to 750 m), and the deep layer (≥750 m). We hypothesize that these layers are related to the traditional Mediterranean circulation scheme which is described by two cells (Manalotte-Rizzoli et al., 1999): the well ventilated surface cell which contains water

BGD
9, 2709–2753, 2012

masses like MAW, WIW, and LIW; and the deep cells which contains the WMDW and TDW in the Western basin, and the $EMDW_{Ard}$ and $EMDW_{Aeg}$ in the Eastern basin. In order to avoid nutrient concentrations close to zero in the surface layer that could prevent the computation of the ratios, all samples with depth <50 m and/or values of AOU (Apparent Oxygen Utilization) <5 µmol kg^{-1} (Western basin) or <10 µmol kg^{-1} (Eastern basin) are ignored.

The results clearly reveal some deviations from the open ocean Redfield et al. (1963) ratios. R_{ON} in the surface/intermediate layer of the Mediterranean Sea is lower (7.16–7.52; see Table 2) than the Redfield value of 8.6, while it is higher in the deep layer (10.3–10.7). The Mediterranean R_{OP} ratios are systematically higher than the Redfield ratio of 138, with ranges of 178–189 and 165–171 for the surface/intermediate and the deep layer, respectively. Using the estimated R_{ON} and R_{OP} values, we also calculate the R_{NP} ratios (Table 2) and obtain ranges of 23.67–26.39 and 15.98–16.02 for the surface/intermediate and the deep layers, respectively. Using the same BOUM data, Pujo-Pay et al. (2010) provided other estimates of the Redfield ratios using either the averaged ratios approach or the approach that uses the slope of the linear regression. Considering only the results of the latter approach (this is the one used in the present study) given by Pujo-Pay et al. (2010), very similar trends are obtained: their R_{NP} ratios increase eastward from 22.9 to 27.9, and they also conclude that the deep water masses that fill both the Western and the Eastern basin are characterized by R_{NP} ratios very close to the canonical Redfield value of 16.

5.1.3 Determination of C_{ANT} using the MIX approach

According to the original approach presented by Goyet et al. (1999), the variation of C_T in seawater can be represented by the equation:

$$C_T^m = C_T^{cir} + C_T^{bio} + C_{ANT} \quad (6)$$

where C_T^m is the measured value of C_T within a sample, C_T^{cir} is the value of C_T that results from the physical processes (mixing, circulation), and C_T^{bio} is the contribution

BGD
9, 2709–2753, 2012

due to the biological processes (respiration/decomposition of organic matter and the $CaCO_3$ formation/dissolution process). Below the mixed layer depth (MLD), C_T^{bio} is parameterized as a function of O_2 and A_T according to the equation of Brewer (1978):

$$C_T^{bio} = R_{CO}\Delta O_2 + \frac{1}{2}\Delta A_T \quad (7)$$

where coefficient R_{CO} is the Redfield ratio ($\psi CO_2/\psi O_2$) which is equal to 0.78 (Brewer, 1978; Goyet and Brewer, 1993; Brewer et al., 1997); and ΔO_2 and ΔA_T represent the variations of O_2 and A_T due to the biological activity, respectively. The conservation equations proposed by Goyet et al. (1999) for non-conservative tracers are used to estimate these terms:

$$O_2 = \sum_{j=1}^{n} k_j O_{2j} + \Delta O_2 \quad (8)$$

$$A_T = \sum_{j=1}^{n} k_j A_{Tj} + \Delta A_T \quad (9)$$

where O_2 and A_T are the sample measured concentrations, the k_j are the proportions of the water sources determined previously with the multi-parameter analysis (see above), and the O_{2j} and A_{Tj} are the typical values for O_2 and A_T within a water source j (see Table 1). From Eqs. (8) and (9), the ΔO_2 and ΔA_T are calculated, from which we can estimate C_T^{bio} using Eq. (7). The contribution due to the physical processes (C_T^{cir}) is computed with the following equation:

$$C_T^{cir} = \sum_{j=1}^{n} k_j C_{Tj}^{cir} \quad (10)$$

where C_{Tj}^{cir} is the pre-industrial value of C_T in each water source j (Table 1). These values are estimated using the CO_2SYS program developed by Lewis and Wallace (1998)

BGD
9, 2709–2753, 2012

with A_{T_j} (total alkalinity of the water source j; see Table 1) and a pCO_2 = 280 µatm (pre-industrial level of the CO_2 partial level) as input variables.

For the MIX approach, the concentration of C_{ANT} is finally estimated from Eq. (6):

$$C_{ANT} = C_T^m - C_T^{cir} - C_T^{bio} \tag{11}$$

5.2 The TrOCA approach

The TrOCA approach is explained in details in Touratier et al. (2007); this simple approach requires only the knowledge of four properties (O_2, A_T, C_T, and θ) in order to provide an accurate estimate of C_{ANT}:

$$C_{ANT} = \frac{TrOCA - TrOCA^0}{a} \tag{12}$$

with:

$$TrOCA = O_2 + a\left[C_T - \frac{1}{2}A_T\right] \tag{13}$$

$$TrOCA^0 = e^{\left(7.511 - \left(1.087\times10^{-2}\right)\theta - \frac{7.81\times10^5}{A_T^2}\right)} \tag{14}$$

$$a = \frac{\psi O_2}{\psi CO_2 + \frac{1}{2}\left(\psi H^+ - \psi HPO_4^{2-}\right)} = 1.279 \tag{15}$$

BGD
9, 2709–2753, 2012

6 Results and comparison of the MIX and TrOCA approaches

The contribution of the 10 water sources (k_j) for the Western and the Eastern basins, computed from the MIX approach, are graphically represented in Figs. 8 and 9, respectively. A value of k_j equal to 1 means that a water sample is exclusively composed by the water source j. As seen in the Western basin (Fig. 8) most k_j values are lower than 0.6, except for the water sources W1 and W7 where they contribute occasionally up to ~80 % of the mixture. The water sources W1, W5, W7, W9, and W10 are well representative for the water masses MAW, WIW, LIW, WMDW, and TDW, respectively. Maxima are located in the expected ranges of depth since the contribution of W1 is the highest in the surface layer, the contributions of W5 and W7 are higher at intermediate depths, and the highest contributions for W9 and W10 are found below 1000 m. The two water sources W2 and W3 (Figs. 3a and 8) are typically representative of the surface water found in an anticylonic gyre which has been intensively sampled during the BOUM cruise (station A, Fig. 1; see Moutin et al., 2012).

For the Eastern basin, the water sources E3, E6, E9, and E10 are typically representative for the water masses MAW, LIW, $EMDW_{Adr}$, and $EMDW_{Aeg}$, respectively. Maxima are also well located in the expected ranges of depth since the contribution of E3 is the highest in the surface layer, the contribution of E6 is strong at intermediate depths, and the main contributions of E9 and E10 are found below 1000 m. The two anticyclonic gyres sampled in the Eastern Mediterranean Sea during the BOUM exercise (stations B and C; see Fig. 1) are best described by the two water sources E1 and E2, respectively (see Figs. 4a and 9). Although the water source E6 is representative for the LIW, it appears from Fig. 9 that water sources E5, E7, and E8 (see θ/S diagram in Fig. 4a) contribute significantly to the formation of LIW.

The distribution of C_{ANT} corresponding to the BOUM 2008 section, calculated from the MIX approach, is shown in Fig. 10a. The C_{ANT} concentration in the Western basin is in average higher (~20 µmol kg^{-1}) than in the Eastern portion of the Mediterranean Sea. All seawater samples collected during the BOUM cruise are contaminated by

BGD
9, 2709–2753, 2012

relatively high levels of anthropogenic CO_2 since the range for the C_{ANT} varies from 48.8 µmol kg^{-1} (this minimum is found at 2000 m in the Ionian Sea) up to 94.7 µmol kg^{-1} (the maximum is found just below the mixed layer depth in the Western basin). Whatever the basin, the intermediate depths are always less contaminated by C_{ANT} than the subsurface or the deep waters. This trend is coherent with the distribution of the O_2 concentration (Fig. 2c) since it reflects the intense events of deep water formation that occur sporadically both in the Eastern (southern regions of the Adriatic and Aegean Seas) and the Western basin (Gulf of Lions). During such processes, detailed for instance in Kress et al. (2003) and Schröder et al. (2006), important volumes of dense waters can rapidly be formed and exported to depth in response to the cooling and/or the evaporation of the surface waters which are characterized by very high levels of O_2 and C_{ANT}.

The distribution of C_{ANT} calculated with the TrOCA approach (Fig. 10b) is both quantitatively and qualitatively very similar to the one computed using the MIX approach (Fig. 10a). As shown in Fig. 11, C_{ANT} computed with the TrOCA approach (C_{ANT}^{TrOCA}) is linearly correlated to C_{ANT} computed with the MIX approach (C_{ANT}^{MIX}) according to the equation $C_{ANT}^{MIX} = 1.03 C_{ANT}^{TrOCA} + 4.22$ ($r^2 = 0.88$; mean and standard deviation of the residuals are 6.05 µmol kg^{-1} and 3.50 µmol kg^{-1}, respectively). We note however two minor differences: (1) the range for the C_{ANT} values computed from TrOCA is slightly lower (~6 µmol kg^{-1}), nevertheless the minima as well as the maxima are located exactly at the same places; (2) the existence of another C_{ANT} minimum in the area of the Sicily Strait that only appears in Fig. 10b (distance from Marseille is ~1400 km). This minimum is absent in the results of the MIX approach (Fig. 10a) since stations 15 to 17 (Sicily Strait; see Fig. 1) were not considered when applying this method.

BGD
9, 2709–2753, 2012

7 Level of acidification reached during the year 2008

The main cause of acidification in the ocean is the accumulation of anthropogenic carbon. Since the beginning of the industrial era it is generally admitted that the pH has already decreased by ~0.1 pH unit in the ocean surface layer (equivalent to an increase of 30 % in the [H+]; Orr et al., 2005; Martin et al., 2008). For the Mediterranean Sea, we expect a relatively high level of acidification due to the high concentration levels recorded for total alkalinity which, combined to a typical Revelle factor of ~9 for the surface Mediterranean waters, allow to absorb relatively more C_{ANT} than in the open ocean (CIESM, 2008; Goyet et al., 2009).

The acidification (ΔpH) along the BOUM section in Fig. 1 is calculated from the difference between the 2008 distribution of pH (pH_{2008}) and the pre-industrial distribution of pH (pH_{preind}):

$$\Delta pH = pH_{2008} - pH_{preind} \quad (16)$$

We then follow the procedure detailed in Touratier and Goyet (2011) to estimate pH_{2008} and pH_{preind}. Using the model CO_2SYS developed by Lewis and Wallace (1998), the pH is accurately estimated from C_T and A_T properties. The pH_{2008} distribution (shown in Fig. 12a) is thus estimated from the 2008 C_T and A_T distributions (Fig. 5a and b, respectively). The pH_{preind} distribution (Fig. 12b) is estimated from the 2008 A_T (Fig. 5b) since we know that this property is not affected by the accumulation of C_{ANT} in seawater. The C_T used to calculate pH_{preind} is the pre-industrial C_T which is computed from the difference between the 2008 C_T distribution (Fig. 5a) and the 2008 C_{ANT} distribution computed from the TrOCA approach (Fig. 10b).

Using Eq. (16), the results for the ΔpH distribution (Fig. 12c) indicate that all water masses in the Mediterranean Sea are already acidified (the range is from −0.148 to −0.061). Waters from the Eastern basin (especially those located in the intermediate layer) appear to be less contaminated than those from the Western basin where ΔpH is often lower than −0.1.

BGD
9, 2709–2753, 2012

8 Discussion and conclusions

Over a period of 7 yr (from the 2001 Meteor cruise to the 2008 BOUM cruise), the range for C_{ANT} slightly increased from 37.5–84.0 µmol kg^{-1} to 46.3–89.6 µmol kg^{-1}. Differences between the minima and the maxima of the previous ranges are 8.8 and 5.6 µmol kg^{-1}, respectively. Such increases are significant since the precision for the MIX and the TrOCA methods are 3.7 µmol kg^{-1} and 6.25 µmol kg^{-1}, respectively (Touratier et al., 2007). Yearly, the C_{ANT} increase amounts to 0.8–1.2 µmol kg^{-1} yr^{-1}, which in terms of acidification corresponds to a mean ΔpH annual decrease of 4.3×10^{-4}–1.8×10^{-3} yr^{-1}. If the highest rate of 1.8×10^{-3} yr^{-1} is assumed for the future, the pH would decrease by 0.1 units after only 56 yr.

The 2008 C_{ANT} and ΔpH distributions globally corroborate those obtained for the year 2001 (published by Touratier and Goyet, 2011). One of the most striking findings of the present study is the great similitude of results between the C_{ANT} estimates computed from the MIX and TrOCA approaches. In spite of their very different structures, hypotheses, and methods of computation (Touratier et al., 2007), the MIX and the TrOCA approaches give almost identical estimates of C_{ANT} for the whole Mediterranean Sea: this is clearly not a coincidence.

Recently, Huertas et al. (2009) and Rivaro et al. (2010) applied the TrOCA approach to estimate C_{ANT} in the Strait of Gibraltar and in different places throughout the Mediterranean Sea, respectively. However, Rivaro et al. (2010) inappropriately applied the TrOCA method in surface waters and estimated C_{ANT} values as high as 135 µmol kg^{-1} in the surface layer of the Eastern basin. This inappropriate maximum was then further used by Schneider et al. (2010) to conclude that the TrOCA approach overestimates C_{ANT}. We remind here that the TrOCA approach cannot be applied in the surface mixed layer (like most other approaches) since the existing biological activities can potentially distort any C_{ANT} estimate. This was a recommendation clearly stated in Touratier et al. (2007).

BGD
9, 2709–2753, 2012

Similarly, Huertas et al. (2009) compares two distributions of C_{ANT} along a longitudinal section throughout the water column from surface to the bottom in the Gibraltar Strait, using the TrOCA approach and the ΔC* method of Gruber et al. (1996). They conclude that C_{ANT} estimated with TrOCA in the Mediterranean Outflowing Water (MOW) is overestimated by ~20 µmol kg^{-1} when compared to the ΔC* estimate. However, the C_{ANT} distributions computed by the two approaches in the surface layer are certainly wrong since biological activities there could induce a large variability in the stoichiometric ratios of nutrients and consequently prevent any application of both TrOCA and ΔC* approaches (the Redfield concept is not viable in this case). Furthermore they explain that the drop of C_T observed in the surface layer is due to the photosynthesis performed by primary producers, thus recognizing the existence of significant biological activities. Moreover they do not provide any scientific argument to explain who the ΔC* approach was suitably well adapted to estimate C_{ANT} in the Mediterranean waters. Contrary to the TrOCA approach, it is well known that input parameters for the ΔC* approach must be adapted for a specific region, but details concerning the determination of these parameters are often lacking. The ΔC* approach applied by Huertas et al. (2009) also depends on the R_{ON} ratio. They set the value of this ratio to 10.6 according to the work of Anderson and Sarmiento (1994) but no sample from the Mediterranean Sea were used in their study. Is this value representative for the MOW? Huertas et al. (2009) consider roughly MOW as a mixture of LIW and WMDW, but the recent work published by Millot (2009) points out that WIW and TDW also contribute significantly to the mixture that exits the Mediterranean Sea through the Gibraltar Strait. From the BOUM 2008 data we learn that R_{ON} = 7.52 for the surface/intermediate waters (Fig. 6a) and R_{ON} = 10.7 for the Western deep water (Fig. 6c). Given that MOW is a mixture of all previous waters (the contribution of each water mass is highly variable both in space and time; see Millot, 2009), it is reasonable to think that the value R_{ON} = 10.6 used by Huertas et al. (2009) for the MOW is overestimated. Like the TrOCA approach, the ΔC* approach has been applied in different areas of the world ocean and several papers have revealed problems inherent

BGD
9, 2709–2753, 2012

to this approach. For instance, in the northern Indian Ocean, Coatanoan et al. (2001) and Touratier et al. (2007) pointed out the incoherence of the C_{ANT} results computed with the ΔC* method within the intermediate waters. For the southern Ocean and the Atlantic Ocean, the paper of Vázquez-Rodríguez et al. (2009) shows that the ΔC* approach underestimated estimates of C_{ANT}. These problems throw doubt on the capacity of the ΔC* approach to estimate C_{ANT} in the Mediterranean Sea.

The very recent paper of Flecha et al. (2012), that used data from the Gibraltar Strait and the Gulf of Cádiz, leads to the same conclusion as Huertas et al. (2009) that TrOCA overestimates C_{ANT} in the MOW. This is not surprising since they use similarly the ΔC* approach and an improved version of it: the so-called φC_T^0 method of Vázquez-Rodríguez et al. (2009). In their introduction, Flecha et al. (2012) affirm that "Current studies have indicated that the TrOCA method considerably overestimates anthropogenic carbon concentrations (Yool et al., 2010)". Here again, this is not scientifically correct. Yool et al. (2010) used a multidisciplinary 3-D model (OCCAM) in order to assess the TrOCA approach applied to the world ocean (marginal seas like the Mediterranean are ignored). Their strategy consists in the utilization of the outputs of their model (which is able to simulates the properties of the carbonate systems and many others) and to use them as input parameters for the TrOCA approach. C_{ANT} estimated with TrOCA by this way is then compared to the C_{ANT} computed (considered as the "true" field of C_{ANT}) with the 3-D OCCAM model. This approach would be valid only if the OCCAM simulated TrOCA input variables (C_T, A_T, O_2, and θ) could be fully validated with the corresponding measured properties. Despite the availability of these measurements from databases like GLODAP (Key et al., 2004), these validations are not presented. In fact, the attempt of validation of OCCAM is only based on a crude comparison between the measured and the simulated concentration of CFC-11. They also try to validate the OCCAM simulated results with those of another model (C_{ANT} from OCCAM is compared to C_{ANT} simulated with the ΔC* method). Why Yool et al. (2010) do not use the numerous measurements available for nutrients, carbonate system properties, salinity, temperature, and many other parameters

BGD
9, 2709–2753, 2012

to objectively validate OCCAM? This appears to be an unavoidable step before publishing any unbiased assessment of the TrOCA approach. Let us remember here that the inter-comparison exercise of Vázquez-Rodríguez et al. (2009), performed in the Atlantic and the southern Oceans, demonstrates that the TrOCA approach never overestimates the distribution of C_{ANT}. Similarly Flecha et al. (2012) also conclude that C_{ANT} estimated with TrOCA, ΔC^*, and φC_T^0 methods are very similar for all water masses except within MOW.

The only comparable study here is that published by Schneider et al. (2010). The authors used the Transit Time Distribution (TTD) approach developed by Waugh et al. (2006) to estimate the C_{ANT} distribution along the Meteor 2001 section. Using exactly the same dataset, Touratier and Goyet (2011) also estimate C_{ANT} but using the TrOCA approach. Despite very similar patterns between the two distributions of C_{ANT}, it is clear that the TTD approach provides lower C_{ANT} estimates (~20 µmol kg^{-1}). Our objective is now to determine what could explain such a difference between the two estimates.

As mentioned by Schneider et al. (2010), in order to apply the TTD approach, a steady state in the deep thermohaline circulation of the Eastern basin must be assumed. After considering the intense modification of the thermohaline circulation that occurred since the beginning of the 1990s due to the Eastern Mediterranean Transient (Roether et al., 1996; Kress et al., 2003), Schneider et al. (2010) admit that the steady state hypothesis for the year 2001 is very doubtful.

Another serious limitation of the TTD approach is the way by which the mixing is parameterized. Schneider et al. (2010) set their ratio Δ/Γ (a measure for mixing) to 1 but they recognize that this value has not yet been tested for its applicability to the Mediterranean Sea.

From the above two arguments, we think that the estimated age of the EMDW (~60 yr) calculated by Schneider et al. (2010) could have been overestimated, with the consequence of a lowered C_{ANT} concentration. During the 2001 Meteor cruise, the bottom layer of the Eastern basin is filled with new EMDW produced during the EMT,

BGD
9, 2709–2753, 2012

which is ~10 yr old. Some mixing of course has occurred with surrounding older water, but the determination of the seawater age remains very uncertain.

Another potential source of error in the TTD approach is that C_{ANT} is derived indirectly from the CFC distribution. Thomas and England (2002) pointed out that CFC storage mainly occurs in colder, high latitude regions, whereas the warmer, low latitude regions of the world ocean play an important role in both storing and absorbing C_{ANT}. In other words, the ratio C_{ANT}/CFC is highly variable and it is consequently a complex matter to estimate the distribution of C_{ANT} from that of CFC. The increase of this ratio with temperature could be either due to an increase of the CO_2 uptake or a reduction of the CO_2 release to the atmosphere at lower latitudes. However the work of Thomas and England (2002) could be easily criticized since C_{ANT} is derived from a model. To remove this uncertainty, we replace C_{ANT} by the $\Delta^{14}C$ tracer since ^{14}C behaves as C_{ANT} (same solubility but with a different history of release to the atmosphere), with the great advantage that this anthropogenic tracer can be accurately measured within water masses. Using the GLODAP world database (Key et al., 2004) we select all samples from which measurements of CFC-11, $\Delta^{14}C$, and temperature are available. We further select only samples from the surface layer (0–100 m) to draw Fig. 13. This figure fully validate the conclusion of Thomas and England (2002) that concentrations of CO_2 anthropogenic tracers like C_{ANT} or $\Delta^{14}C$ cannot be easily deduced from that of CFC.

Going from the Gibraltar Strait to the Levantin basin, the Mediterranean Sea surface waters are characterized by strong gradients for many of its properties (temperature, salinity, A_T, C_T, Revelle factor, etc.). Schneider et al. (2010) do not describe the potential impact of these gradients on the appropriateness of the TTD approach to estimate C_{ANT} from the CFC distribution. For instance, given the very high temperature reached by the surface water during the 2001 Meteor cruise (up to 26 °C) or the 2008 BOUM cruise (up to 27.64 °C), the content of C_{ANT} is expected to be very high relative to the CFC content. This could partly explain why C_{ANT} estimated with TTD in the Mediterranean Sea is probably underestimated. It is also well known that partial pressure of CFC decreases slowly in the atmosphere since the period 1992–1995, while the partial

BGD
9, 2709–2753, 2012

pressure of CO_2 is always increasing. How the TTD approach deals with such diverging trends in the time evolution of the two tracers?

In addition to the known general problems inherent to the approaches that use CFCs to estimate C_{ANT} (see the above discussion), this study further shows that the TTD and all CFCs based approaches (such as the ΔC^* or the φC_T^0 approach) are not suitable to estimate C_{ANT} in the Mediterranean Sea waters. Only carbon based approaches such as the MIX or TrOCA method can appropriately deal with the specificities of each particular ocean basin and provide meaningful estimates of C_{ANT} throughout the whole ocean (including the Mediterranean Sea) below the wintertime mixed layer. Wherever the TrOCA method has been used, its C_{ANT} results provided very similar results compared to those of the MIX approach that requires additional knowledge on the physical properties of the studied ocean area. Here again the results prove the robustness of the "simple" TrOCA approach.

Thus, this study indicates that the Mediterranean Sea waters (below the mixed layer) are highly contaminated with anthropogenic carbon ($>46.3\,\mu mol\,kg^{-1}$). Consequently, the Mediterranean Sea is one of the most acidified marine ecosystems ($0.061 < \Delta pH < 0.148$).

Acknowledgements. We would like to thank the Chief Scientist (Thierry Moutin), the scientists and crew who participated to the 2008 BOUM cruise. A special thanks for Karine Leblanc who provides the silicates data. This is a contribution of the BOUM (Biogeochemistry from the Oligotrophic to the Ultraoligotrophic Mediterranean) experiment (http://www.com.univ-mrs.fr/BOUM) of the French national LEFE-CYBER program, the European IP SESAME and the international IMBER project.This work was also funded by the EC FP7 "Mediterranean Sea Acidification in a changing climate" project (MedSea; grant agreement 265103).

References

Álvarez, M., Lo Monaco, C., Tanhua, T., Yool, A., Oschlies, A., Bullister, J. L., Goyet, C., Metzl, N., Touratier, F., McDonagh, E., and Bryden, H. L.: Estimating the storage of anthropogenic

BGD
9, 2709–2753, 2012

carbon in the subtropical Indian Ocean: a comparison of five different approaches, Biogeosciences, 6, 681–703, doi:10.5194/bg-6-681-2009, 2009.
Anderson, L. A. and Sarmiento, J. L.: Redfield ratios of remineralization determined by nutrient data analysis, Global Biogeochem. Cy., 8, 65–80, doi:199410.1029/93GB03318, 1994.
Brewer, P. G.: Direct observation of the oceanic CO_2 increase, Geophys. Res. Lett., 5, 997–1000, doi:197810.1029/GL005i012p00997, 1978.
Brewer, P. G., Goyet, C., and Friederich, G.: Direct observation of the oceanic CO_2 increase?revisited, P. Natl. Acad. Sci., 94, 8308–8313, 1997.
Broecker, W. S.: "NO", a conservative water-mass tracer, Earth Planet. Sci. Lett., 23, 100–107, doi:10.1016/0012-821X(74)90036-3, 1974.
CIESM: Impacts of acidification on biological, chemical and physical systems in the Mediterranean and Black Seas, CIESM Workshop Monographs, Briand F., 2008.
Coatanoan, C., Goyet, C., Gruber, N., Sabine, C. L., and Warner, M.: Comparison of two approaches to quantify anthropogenic CO_2 in the ocean: Results from the northern Indian Ocean, Global Biogeochem. Cy., 15, 11–25, doi:200110.1029/1999GB001200, 2001.
Crombet, Y., Leblanc, K., Quéguiner, B., Moutin, T., Rimmelin, P., Ras, J., Claustre, H., Leblond, N., Oriol, L., and Pujo-Pay, M.: Deep silicon maxima in the stratified oligotrophic Mediterranean Sea, Biogeosciences, 8, 459–475, doi:10.5194/bg-8-459-2011, 2011.
DOE: Handbook and methods for the analysis of the various parameters of the carbon dioxide system in seawater, 1994.
Flecha, S., Pérez, F. F., Navarro, G., Ruiz, J., Olivé, I., Rodríguez-Gálvez, S., Costas, E., and Huertas, I. E.: Anthropogenic carbon inventory in the Gulf of Cádiz, J. Mar. Syst., 92, 67–75, doi:10.1016/j.jmarsys.2011.10.010, 2012.
Gerber, M., Joos, F., Vázquez-Rodríguez, M., Touratier, F., and Goyet, C.: Regional air-sea fluxes of anthropogenic carbon inferred with an Ensemble Kalman Filter, Global Biogeochem. Cy., 23, GB1013, doi:200910.1029/2008GB003247, 2009.
Goyet, C. and Brewer, P. G.: Biochemical properties of the oceanic carbon cycle, in: Modelling oceanic climate interactions, edited by: Willebrand J. and Anderson D. L. T., Springer Verlag, 1993.
Goyet, C. and Touratier, F.: Challenges for present and future estimates of anthropogenic carbon in the Indian Ocean, Geophys. Mono. Ser., 185, 231–237, 2009.
Goyet, C., Coatanoan, C., Eischeid, G., Amaoka, T., Okuda, K., Healy, R., and Tsunogai, S.: Spatial variation of total CO₂ and total alkalinity in the northern Indian

BGD
9, 2709–2753, 2012

Ocean: A novel approach for the quantification of anthropogenic CO₂ in seawater, J. Mar. Res., 57, 135–163, doi:10.1357/002224099765038599, 1999.
Goyet, C., Ito Gonçalves, R., and Touratier, F.: Anthropogenic carbon distribution in the eastern South Pacific Ocean, Biogeosciences, 6, 149–156, doi:10.5194/bg-6-149-2009, 2009.
Gruber, N., Sarmiento, J. L., and Stocker, T. F.: An improved method for detecting anthropogenic CO_2 in the oceans, Global Biogeochem. Cy., 10, 809–837, doi:199610.1029/96GB01608, 1996.
Huertas, I. E., Ríos, A. F., García-Lafuente, J., Makaoui, A., Rodríguez-Gálvez, S., Sánchez-Román, A., Orbi, A., Ruíz, J., and Pérez, F. F.: Anthropogenic and natural CO_2 exchange through the Strait of Gibraltar, Biogeosciences, 6, 647–662, doi:10.5194/bg-6-647-2009, 2009.
Key, R. M., Kozyr, A., Sabine, C. L., Lee, K., Wanninkhof, R., Bullister, J. L., Feely R. A., Millero, F. J., Mordy, C., and Peng, T.-H.: A global ocean carbon climatology: Results from Global Data Analysis Project (GLODAP), Global Biogeochem. Cy., 18, GB4031, doi:200410.1029/2004GB002247, 2004.
Klein, B., Roether, W., Manca, B. B., Bregant, D., Beitzel, V., Kovacevic, V., and Luchetta, A.: The large deep water transient in the Eastern Mediterranean, Deep Sea Res. I, 46, 371–414, doi:10.1016/S0967-0637(98)00075-2, 1999.
Kress, N., Manca, B. B., Klein, B., and Deponte, D.: Continuing influence of the changed thermohaline circulation in the eastern Mediterranean on the distribution of dissolved oxygen and nutrients: Physical and chemical characterization of the water masses, J. Geophys. Res., 108, 8109, doi:10.1029/2002JC001397, 2003.
Lascaratos, A., Roether, W., Nittis, K., and Klein, B.: Recent changes in deep water formation and spreading in the eastern Mediterranean Sea: a review, Progr. Oceanogr., 44, 5–36, doi:10.1016/S0079-6611(99)00019-1, 1999.
Lewis, E. and Wallace, D. W. R.: Programdeveloped for CO_2 system calculations, ORNL/CDIAC, 1998.
Mackas, D. L., Denman, K. L., and Bennett, A. F.: Least Squares Multiple Tracer Analysis of Water Mass Composition, J. Geophys. Res., 92, 2907–2918, doi:198710.1029/JC092iC03p02907, 1987.
Malanotte-Rizzoli, P., Manca, B. B., d' Alcala, M. R., Theocharis, A., Brenner, S., Budillon, G., and Ozsoy, E.: The Eastern Mediterranean in the 80s and in the 90s: the big transition in the intermediate and deep circulations, Dynam. Atmos. Oceans, 29, 365–395,

BGD
9, 2709–2753, 2012

doi:10.1016/S0377-0265(99)00011-1, 1999.
Martin, S., Gazeau, F., Orr, J., and Gattuso, J. P.: Ocean acidification and its consequences, 5–16, *Dans* Lettre pigb-pmrc, 2008.
Millot, C: Another description of the Mediterranean Sea outflow, Prog. Oceanogr., 82, 101–124, doi:10.1016/j.pocean.2009.04.016, 2009.
Millot, C., Candela, J., Fuda, J.-L., and Tber, Y.: Large warming and salinification of the Mediterranean outflow due to changes in its composition, Deep Sea Res. I, 53, 656–666, doi:10.1016/j.dsr.2005.12.017, 2006.
Moutin, T., Van Wambeke, F., and Prieur, L.: The Biogeochemistry from the Oligotrophic to the Ultraoligotrophic Mediterranean (BOUM) experiment, Biogeosciences Discuss., 8, 8091–8160, doi:10.5194/bgd-8-8091-2011, 2011.
Orr, J. C., Fabry, V. J., Aumont, O., Bopp, L., Doney, S. C., Feely, R. A., Gnanadesikan, A., Gruber, N., Ishida, A., Joos, F., Key, R. M., Lindsay, K., Maier-Reimer, E., Matear, R., Monfray, P., Mouchet, A., Najjar, R. G., Plattner, G.-K., Rodgers, K. B., Sabine, C. L., Sarmiento, J. L., Schlitzer, R., Slater, R. D., Totterdell, I. J., Weirig, M.-F., Yamanaka, Y., and Yool, A.: Anthropogenic ocean acidification over the twenty-first century and its impact on calcifying organisms, Nature, 437, 681–686, doi:10.1038/nature04095, 2005.
Pujo-Pay, M., Conan, P., Oriol, L., Cornet-Barthaux, V., Falco, C., Ghiglione, J.-F., Goyet, C., Moutin, T., and Prieur, L.: Integrated survey of elemental stoichiometry (C, N, P) from the western to eastern Mediterranean Sea, Biogeosciences, 8, 883–899, doi:10.5194/bg-8-883-2011, 2011.
Redfield, A. C., Ketchum, B. H., and Richards, F. A.: The influence of organisms on the composition of seawater, 26–77, in: The Sea, Hill M. N., 1963.
Rivaro, P., Messa, R., Massolo, S., and Frache, R.: Distributions of carbonate properties along the water column in the Mediterranean Sea: Spatial and temporal variations, Mar. Chem., 121, 236–245, doi:10.1016/j.marchem.2010.05.003, 2010.
Roether, W., Manca, B. B., Klein, B., Bregant, D., Georgopoulos, D., Beitzel, V., Kovaćevič, V., and Luchetta, A.: Recent Changes in Eastern Mediterranean Deep Waters, Science, 271, 333–335, doi:10.1126/science.271.5247.333, 1996.
Roether, W., Beitzel, V., Sültenfuß, J., and Putzka, A.: The Eastern Mediterranean tritium distribution in 1987, J. Mar. Syst., 20, 49–61, doi:10.1016/S0924-7963(98)00070-0, 1999.
Rubino, A. and Hainbucher, D.: A large abrupt change in the abyssal water masses of the eastern Mediterranean, Geophys. Res. Lett., 34, L23607, doi:200710.1029/2007GL031737,

BGD
9, 2709–2753, 2012

2007.
Sandrini, S., Ait-Ameur, N., Rivaro, P., Massolo, S., Touratier, F., Tositti, L., and Goyet, C.: Anthropogenic Carbon Distribution in the Ross Sea, Antarctica, Antarctic Sci., 19, 395–407, doi:10.1017/S0954102007000405, 2007.
Schneider, A., Tanhua, T., Körtzinger, A., and Wallace, D. W. R.: High anthropogenic carbon content in the eastern Mediterranean, J. Geophys. Res., 115, C12050, doi:10.1029/2010JC006171, 2010.
Schneider, A., Wallace, D. W. R., and Körtzinger, A.: Alkalinity of the Mediterranean Sea, Geophys. Res. Lett., 34, L15608, doi:10.1029/2006GL028842, 2007.
Schröder, K., Gasparini, G. P., Tangherlini, M., and Astraldi, M.: Deep and intermediate water in the western Mediterranean under the influence of the Eastern Mediterranean Transient, Geophys. Res. Lett., 33, L21607, doi:10.1029/2006GL027121, 2006.
Theocharis, A., Klein, B., Nittis, K., and Roether, W.: Evolution and status of the Eastern Mediterranean Transient (1997–1999), J. Mar. Syst., 33–34 91–116, doi:10.1016/S0924-7963(02)00054-4, 2002.
Thomas, H. and England, M.: Different oceanic features of anthropogenic CO_2 and CFCs, Naturwissenschaften, 89, 399–403, doi:10.1007/s00114-002-0348-5, 2002.
Tomczak, M.: An analysis of mixing in the frontal zone of South and North Atlantic Central Water off North-West Africa, Prog. Oceanogr., 10, 173–192, doi:10.1016/0079-6611(81)90011-2, 1981.
Touratier, F. and Goyet, C.: Applying the new TrOCA approach to assess the distribution of anthropogenic CO_2 in the Atlantic Ocean, J. Mar. Syst., 46, 181–197, doi:10.1016/j.jmarsys.2003.11.020, 2004.
Touratier, F. and Goyet, C.: Decadal evolution of anthropogenic CO_2 in the northwestern Mediterranean Sea from the mid-1990s to the mid-2000s, Deep Sea Res. I, 56, 1708–1716, doi:10.1016/j.dsr.2009.05.015, 2009.
Touratier, F. and Goyet, C.: Impact of the Eastern Mediterranean Transient on the distribution of anthropogenic CO_2 and first estimate of acidification for the Mediterranean Sea, Deep Sea Res. I, 58, 1–15, doi:10.1016/j.dsr.2010.10.002, 2011.
Touratier, F., Goyet, C., Coatanoan, C., and Andrié, C.: Assessments of anthropogenic CO_2 distribution in the tropical Atlantic Ocean, Deep Sea Res. I, 52, 2275–2284, doi:10.1016/j.dsr.2005.09.001, 2005.

BGD
9, 2709–2753, 2012

Touratier, F., Azouzi, L., and Goyet, C.: CFC-11, Δ14C and 3H tracers as a means to assess anthropogenic CO_2 concentrations in the ocean, Tellus B, 59, 318–325, doi:10.1111/j.1600-0889.2006.00247.x, 2007.

Vázquez-Rodríguez, M., Touratier, F., Lo Monaco, C., Waugh, D. W., Padin, X. A., Bellerby, R. G. J., Goyet, C., Metzl, N., Ríos, A. F., and Pérez, F. F.: Anthropogenic carbon distributions in the Atlantic Ocean: data-based estimates from the Arctic to the Antarctic, Biogeosciences, 6, 439–451, doi:10.5194/bg-6-439-2009, 2009.

Waugh, D. W., Hall, T. M., McNeil, B. I., Key, R., and Matear, R. J.: Anthropogenic CO_2 in the oceans estimated using transit time distributions, Tellus B, 58, 376–389, doi:10.1111/j.1600-0889.2006.00222.x, 2006.

Yool, A., Oschlies, A., Nurser, A. J. G., and Gruber, N.: A model-based assessment of the TrOCA approach for estimating anthropogenic carbon in the ocean, Biogeosciences, 7, 723–751, doi:10.5194/bg-7-723-2010, 2010.

BGD
9, 2709–2753, 2012

Table 1. Water sources physical and chemical properties used by the MIX approach in the two basins of the Mediterranean Sea.

Indice j	Water Source	Depth (m)	Temperature (°C)	S_j	Θ_j (°C)	NO_{3j} (μmol kg^{-1})	PO_{4j} (μmol kg^{-1})	$SiOH_{4j}$ (μmol kg^{-1})	O_{2j} (μmol kg^{-1})	A_{Tj} (μmol kg^{-1})	C_{Tj}^{cir} (μmol kg^{-1})
					Western Basin						
1	W1	50	17.21	37.269	17.20	0.00	0.002	0.90	240.8	2471.7	2103.0
2	W2	50	15.96	37.240	15.95	0.00	0.007	0.78	248.7	2465.3	2110.8
3	W3	149	14.30	37.687	14.28	1.10	0.030	0.75	234.8	2512.3	2163.5
4	W4	50	15.12	38.163	15.12	0.05	0.032	0.89	259.0	2556.3	2186.8
5	W5	148	13.15	38.315	13.13	5.48	0.165	2.73	216.5	2558.9	2209.5
6	W6	199	13.24	38.401	13.21	7.59	0.276	3.92	203.5	2583.7	2228.2
7	W7	496	14.15	38.853	14.07	5.69	0.192	7.45	181.8	2604.3	2233.9
8	W8	2965	13.86	38.710	13.38	4.91	0.142	9.11	195.4	2634.3	2276.2
9	W9	1483	13.08	38.459	12.86	8.78	0.383	8.47	190.0	2588.5	2240.4
10	W10	2839	13.31	38.472	12.86	8.61	0.391	8.22	196.2	2595.3	2250.9
					Eastern Basin						
1	E1	50	18.40	38.082	18.39	0.00	0.001	0.70	242.1	2516.7	2121.4
2	E2	50	18.69	39.410	18.68	0.00	0.009	0.83	238.7	2625.0	2194.7
3	E3	73	15.73	37.618	15.72	0.00	0.001	0.93	239.7	2506.0	2143.6
4	E4	174	15.59	38.436	15.56	2.37	0.102	1.67	205.9	2585.8	2204.3
5	E5	124	17.45	39.398	17.42	0.65	0.051	0.76	213.6	2660.7	2236.9
6	E6	248	16.25	39.163	16.21	0.96	0.013	1.13	220.6	2617.9	2218.6
7	E7	496	14.15	38.853	14.07	5.69	0.192	7.45	181.8	2604.3	2233.9
8	E8	173	15.17	39.045	15.14	3.34	0.090	3.09	204.9	2614.2	2227.8
9	E9	2965	13.86	38.710	13.38	4.91	0.142	9.11	195.4	2634.3	2276.2
10	E10	2222	14.00	38.789	13.64	4.84	0.167	8.00	189.3	2617.4	2256.2

BGD
9, 2709–2753, 2012

Table 2. Results obtained for the orthogonal regressions of the nutrients (NO_3 and PO_4) versus O_2 used to estimate the ratios R_{ON} and R_{OP}. Ratio R_{NP} is calculated from the ratio R_{OP}/R_{ON}.

Western Basin	50 m ≤ Depth < 750 m AOU > 5 µmol kg^{-1}			Depth ≥ 750 m		
	R_{ON}	R_{OP}	R_{NP}	R_{ON}	R_{OP}	R_{NP}
Value	7.52	178	23.67	10.7	171	15.98
Number of points	183	182		35	37	
Mean of the residuals	0.003	0.004		0.03	0.01	
Standard deviation of the residuals	7.41	7.20		2.52	2.88	
Pearson correlation coefficient	0.96	0.96		0.69	0.71	
99 % confidence interval	[7.24; 7.79]	[171; 184]		[4.80; 16.6]	[76.8; 266]	
Eastern Basin	50 m ≤ Depth < 750 m AOU > 10 µmol kg^{-1}			Depth ≥ 750 m		
	R_{ON}	R_{OP}	R_{NP}	R_{ON}	R_{OP}	R_{NP}
Value	7.16	189	26.39	10.3	165	16.02
Number of points	272	264		68	68	
Mean of the residuals	0.04	0.04		0.02	0.0003	
Standard deviation of the residuals	3.33	4.84		2.67	2.74	
Pearson correlation coefficient	0.97	0.93		0.89	0.85	
99 % confidence interval	[6.75; 7.58]	[178; 201]		[7.8; 12.4]	[125; 199]	

BGD
9, 2709–2753, 2012

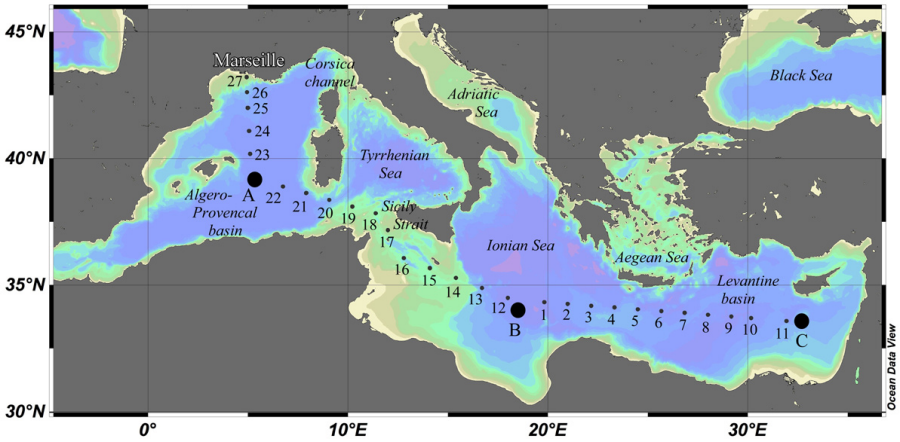

Fig. 1. Map of the 2008 BOUM cruise in the Mediterranean Sea. Short-term stations are indicated by numbers (from 1 to 27); the three long-term stations are referred as A, B, and C.

BGD
9, 2709–2753, 2012

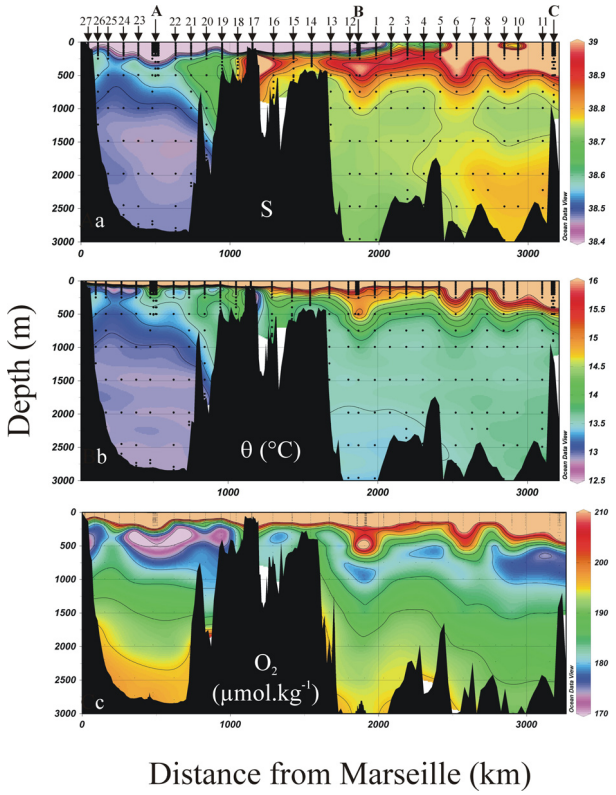

Fig. 2. Property distributions along the 2008 BOUM transect going from Marseille (France; Station 27; distance is 0 km) to the Levantine Basin (south of Cyprus Island; Station C; distance from Marseille is ~3200 km). **(a)** Salinity (S); **(b)** potential temperature (θ; °C); and **(c)** concentration of dissolved oxygen (O_2; µmol kg^{-1}). Stations along the transect are indicated above panel **(a)**.

BGD
9, 2709–2753, 2012

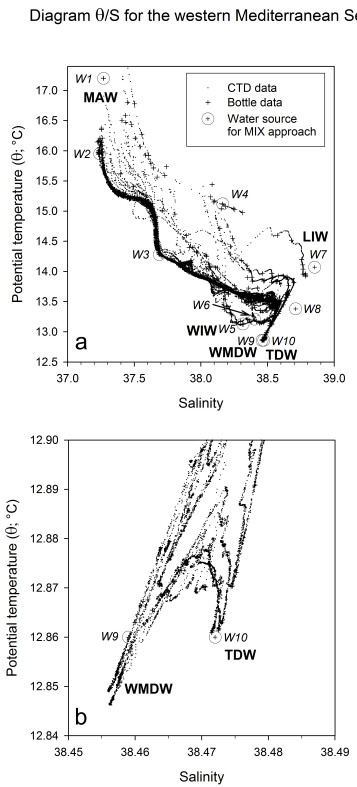

Fig. 3. Diagram θ/S for the Western Mediterranean Sea where CTD and bottle data are all represented. The main water masses (MAW, WIW, LIW, TDW, and WMDW) described in the text and the 10 water sources (from W1 to W10) used by the MIX approach are also indicated. Panel **(b)** is a zoom of **(a)** in order to better visualize WMDW and TDW.

BGD
9, 2709–2753, 2012

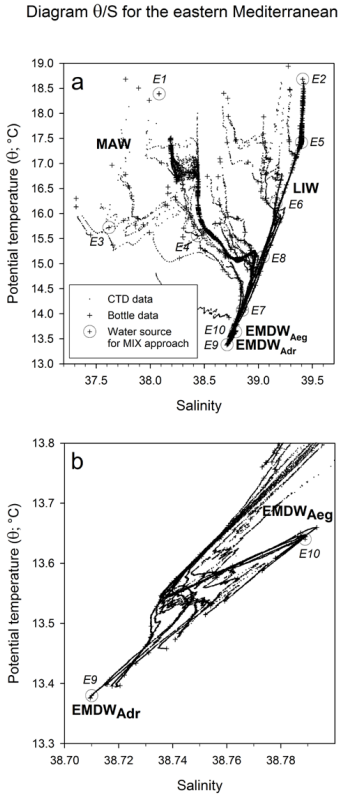

Fig. 4. Diagram *θ/S* for the Eastern Mediterranean Sea where CTD and bottle data are all represented. The main water masses (MAW, LIW, $EMDW_{Adr}$, and $EMDW_{Aeg}$) described in the text and the 10 water sources (from E1 to E10) used by the MIX approach are also indicated. Panel **(b)** is a zoom of **(a)** in order to better visualize $EMDW_{Adr}$ and $EMDW_{Aeg}$.

BGD
9, 2709–2753, 2012

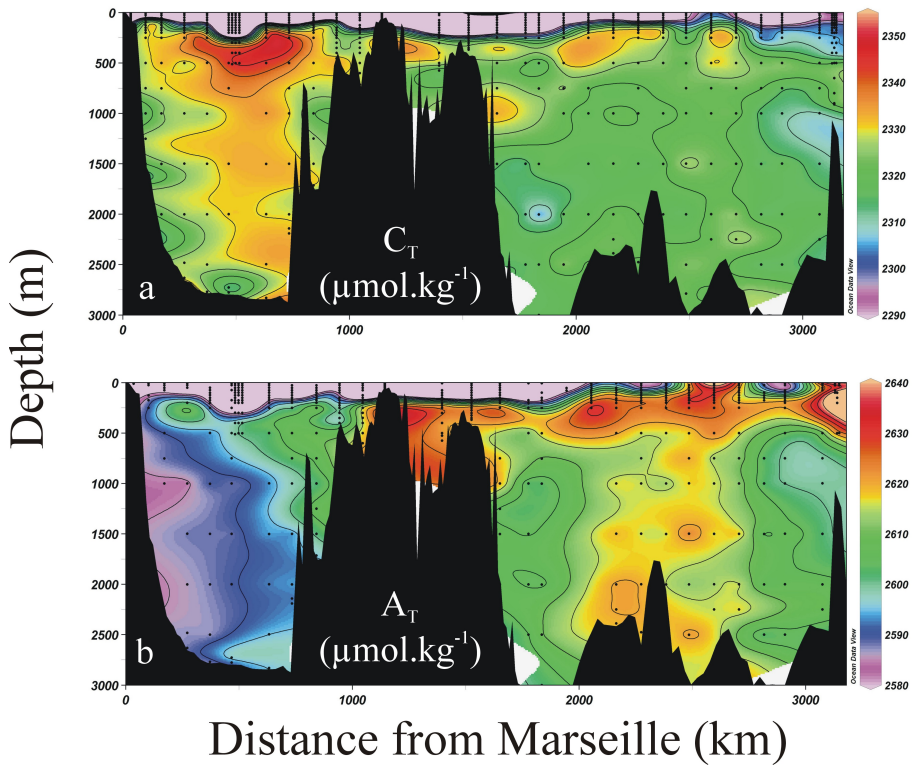

Fig. 5. (a) Distribution of the total dissolved inorganic carbon (C_T, µmol kg^{-1}); **(b)** distribution of the total alkalinity (A_T; µmol kg^{-1}).

BGD
9, 2709–2753, 2012

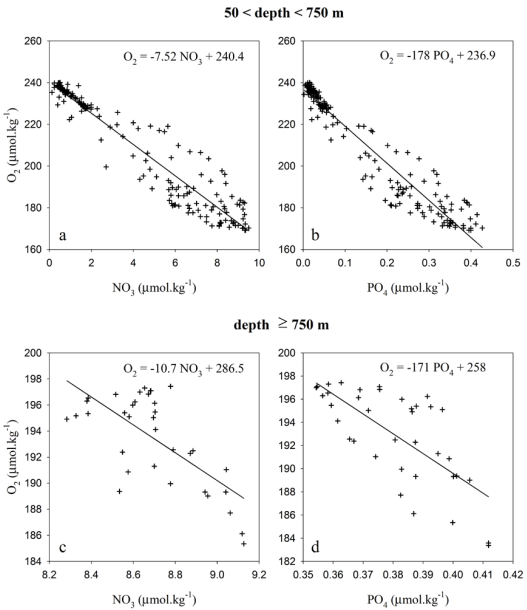

Fig. 6. Relationships between nutrients (NO_3 and PO_4) and O_2, using data from the Western Mediterranean Sea. **(a)** Relationship between NO_3 and O_2 in the layer 50–750 m; **(b)** relationship between PO_4 and O_2 in the layer 50–750 m; **(c)** relationship between NO_3 and O_2 for depths >750 m; **(d)** relationship between PO_4 and O_2 for depths >750 m. All panels include the linear regression with the corresponding equation. Details about these regressions are given in the text and Table 2.

BGD
9, 2709–2753, 2012

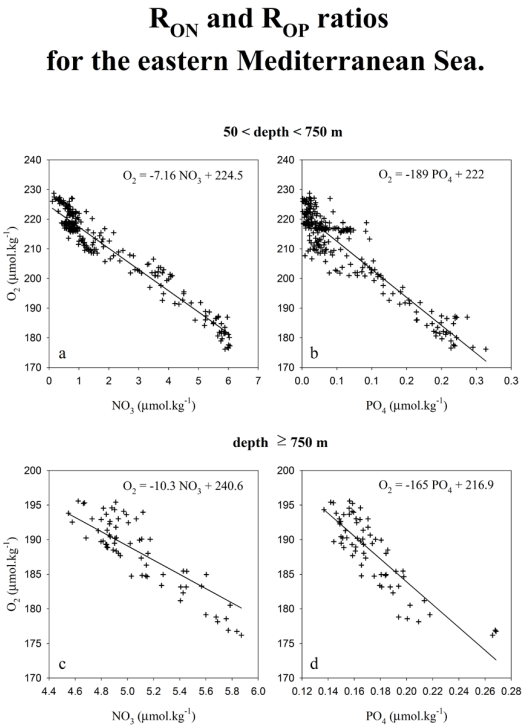

Fig. 7. Relationships between nutrients (NO_3 and PO_4) and O_2, using data from the Eastern Mediterranean Sea. **(a)** Relationship between NO_3 and O_2 in the layer 50–750 m; **(b)** relationship between PO_4 and O_2 in the layer 50–750 m; **(c)** relationship between NO_3 and O_2 for depths >750 m; **(d)** relationship between PO_4 and O_2 for depths >750 m. All panels include the linear regression with the corresponding equation. Details about these regressions are given in the text and Table 2.

BGD
9, 2709–2753, 2012

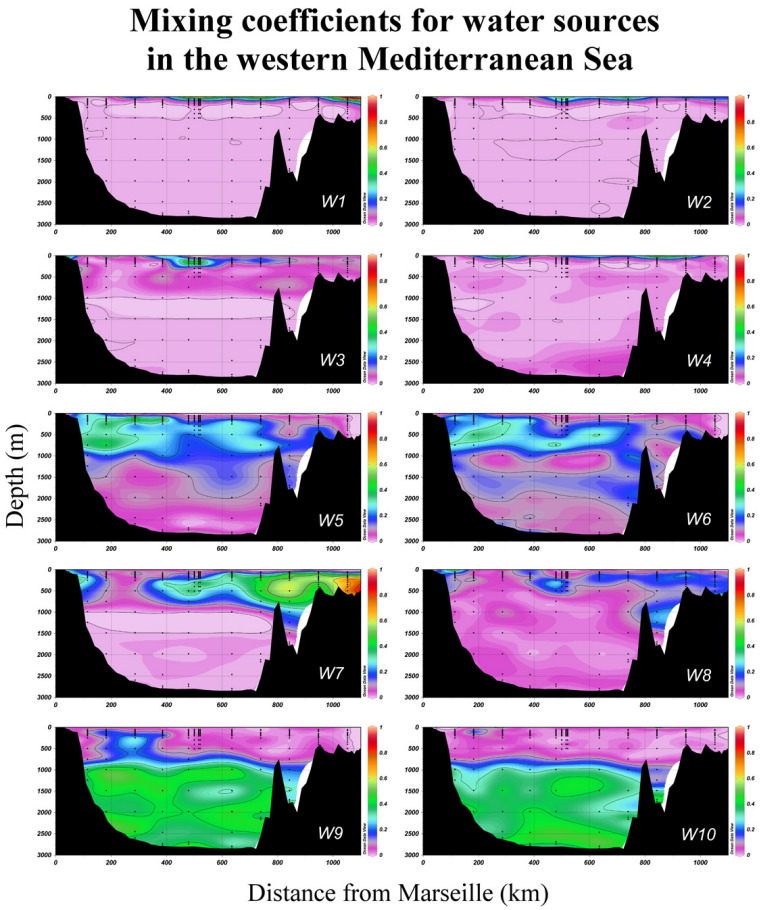

Fig. 8. Results of the MIX approach. Distribution of the mixing coefficient (k_j) of each water source (from W1 to W10) in the Western Mediterranean Sea.

BGD
9, 2709–2753, 2012

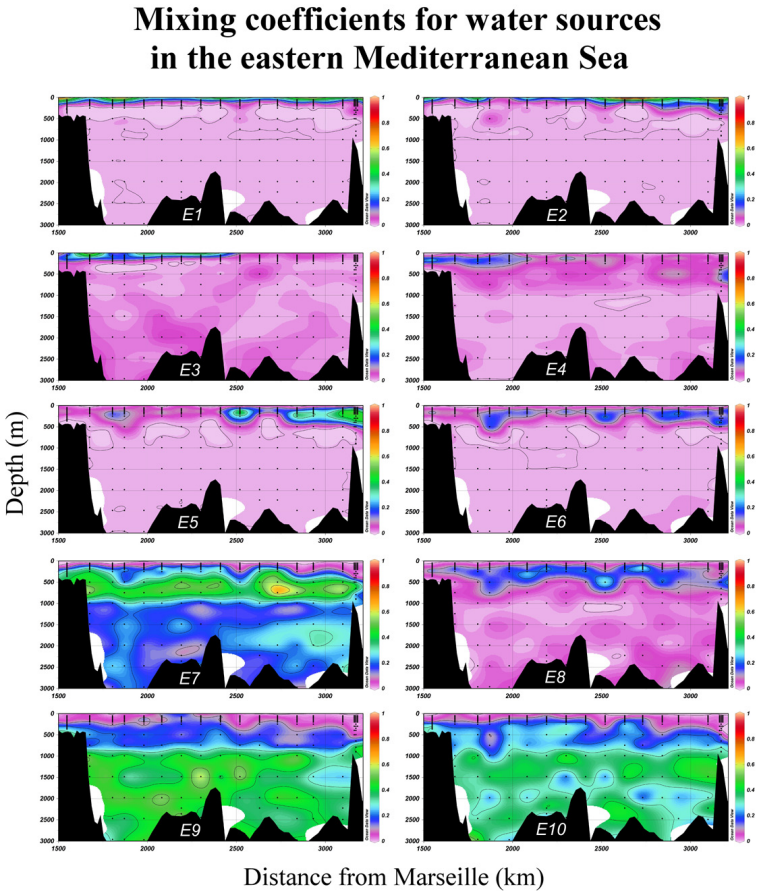

Fig. 9. Results of the MIX approach. Distribution of the mixing coefficient (k_j) of each water source (from E1 to E10) in the Eastern Mediterranean Sea.

BGD
9, 2709–2753, 2012

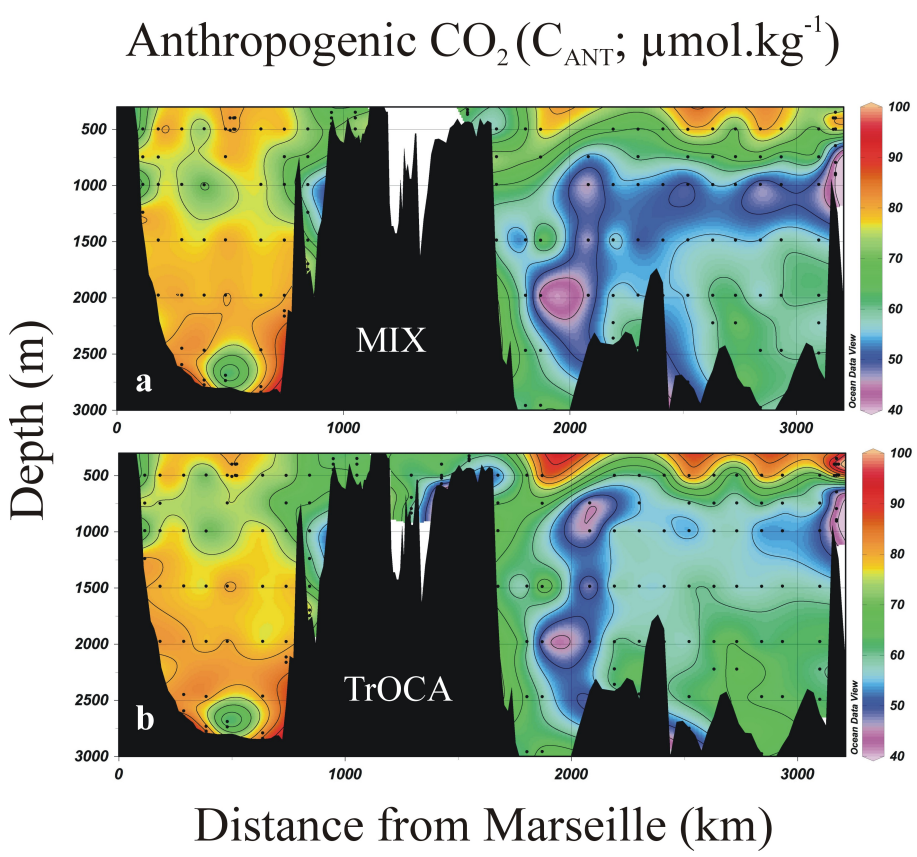

Fig. 10. Distributions of anthropogenic CO_2 (C_{ANT}; µmol kg^{-1}): **(a)** using the MIX approach; **(b)** using the TrOCA approach.

BGD
9, 2709–2753, 2012

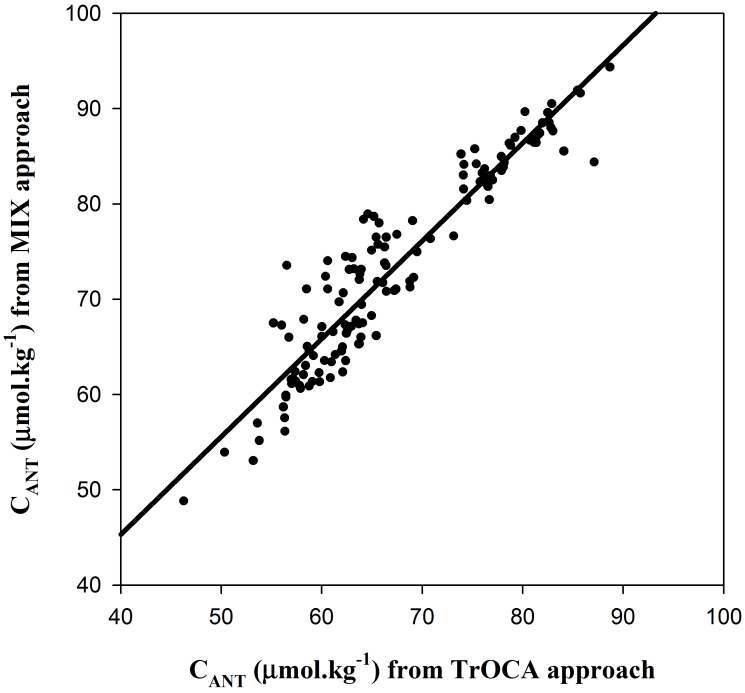

Fig. 11. Relationship and linear regression between C_{ANT} estimated with MIX and C_{ANT} estimated with TrOCA.

BGD
9, 2709–2753, 2012

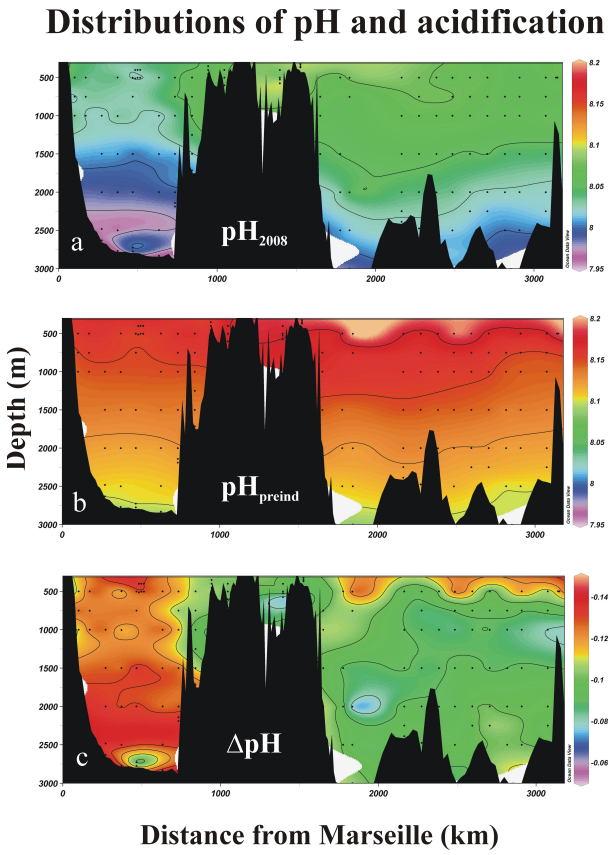

Fig. 12. Distributions of **(a)** pH estimated from the 2008 BOUM dataset; **(b)** pre-industrial pH; and **(c)** acidification (ΔpH) for the year 2008. Details concerning the computation of these distributions are given in the text.

BGD
9, 2709–2753, 2012

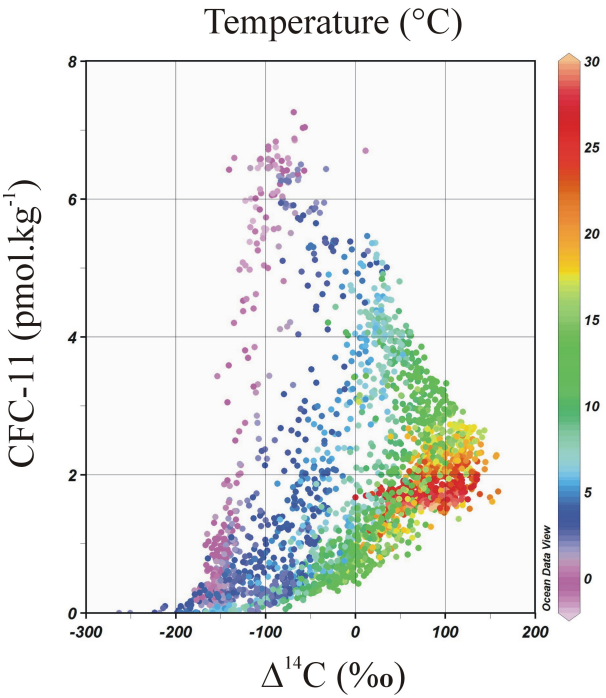

Fig. 13. Picture of the complex relationship between two anthropogenic tracers (CFC-11, pmol kg^{-1}; $\Delta^{14}C$, ‰) and the temperature. These data originates from the world database GLODAP (Key et al., 2004). Only data from the surface layer (0–100 m) have been selected.

BGD
9, 2709–2753, 2012